WILEY

RESEARCH ARTICLE

Proactive and reactive cognitive control rely on flexible use of the ventrolateral prefrontal cortex

Sephira G. Ryman[1,2] | Ansam A. El Shaikh[2] | Nicholas A. Shaff[2] | Faith M. Hanlon[2] | Andrew B. Dodd[2] | Christopher J. Wertz[2] | Josef M. Ling[2] | Deanna M. Barch[3] | Shannon F. Stromberg[4] | Denise S. Lin[4] | Swala Abrams[4] | Andrew R. Mayer[1,2,4,5] (ORCID)

[1]Department of Psychology, University of New Mexico, Albuquerque, New Mexico

[2]The Mind Research Network/Lovelace Biomedical and Environmental Research Institute, Albuquerque, New Mexico

[3]Department of Psychological and Brain Sciences, Washington University in St. Louis, St. Louis, Missouri

[4]Department of Psychiatry, University of New Mexico School of Medicine, Albuquerque, New Mexico

[5]Department of Neurology, University of New Mexico School of Medicine, Albuquerque, New Mexico

Correspondence

Andrew Mayer, PhD, The Mind Research Network, Pete & Nancy Domenici Hall, 1101 Yale Boulevard NE, Albuquerque, NM 87106, USA.
Email: amayer@mrn.org

Funding information

National Institute of Mental Health, Grant/Award Number: 1R01MH101512-03; National Institutes of Health

Abstract

The role of ventral versus dorsolateral prefrontal regions in instantiating proactive and reactive cognitive control remains actively debated, with few studies parsing cue versus probe-related activity. Rapid sampling (460 ms), long cue–probe delays, and advanced analytic techniques (deconvolution) were therefore used to quantify the magnitude and variability of neural responses during the AX Continuous Performance Test (AX-CPT; $N = 46$) in humans. Behavioral results indicated slower reaction times during reactive cognitive control (AY trials) in conjunction with decreased accuracy and increased variability for proactive cognitive control (BX trials). The anterior insula/ventrolateral prefrontal cortex (aI/VLPFC) was commonly activated across comparisons of both proactive and reactive cognitive control. In contrast, activity within the dorsomedial and dorsolateral prefrontal cortex was limited to reactive cognitive control. The instantiation of proactive cognitive control during the probe period was also associated with sparse neural activation relative to baseline, potentially as a result of the high degree of neural and behavioral variability observed across individuals. Specifically, the variability of the hemodynamic response function (HRF) within motor circuitry increased after the presentation of B relative to A cues (i.e., late in HRF) and persisted throughout the B probe period. Finally, increased activation of right aI/VLPFC during the cue period was associated with decreased motor circuit activity during BX probes, suggesting a possible role for the aI/VLPFC in proactive suppression of neural responses. Considered collectively, current results highlight the flexible role of the VLPFC in implementing cognitive control during the AX-CPT task but suggest large individual differences in proactive cognitive control strategies.

KEYWORDS

AX-CPT, proactive cognitive control, reactive cognitive control, ventrolateral prefrontal cortex

1 | INTRODUCTION

The dual mechanisms of control (DMC) theory suggest that cognitive control is instantiated through either proactive or reactive processes (Braver, 2012; Braver, Paxton, Locke, & Barch, 2009). Proactive cognitive control requires an individual to maintain goal-relevant information over sustained periods of time following an external or internal cue and is therefore metabolically expensive (Braver et al., 2009). In contrast, corrective actions to emergent and potentially competing sensory or motor representations

(i.e., reactive cognitive control) may require fewer neuronal resources due to the brief nature of the response (Morishima, Okuda, & Sakai, 2010). It is well known that medial and lateral prefrontal cortex are critically involved in both mechanisms of cognitive control (Miller & Cummings, 2017; Niendam et al., 2012). However, the exact role of these regions, their associated patterns of neuronal activity (i.e., sustained vs. transitory) and how they are affected by individual differences (i.e., variability in execution) remain actively debated (Irlbacher, Kraft, Kehrer, & Brandt, 2014; Redick, 2014).

The dorsolateral (DLPFC) and ventrolateral (VLPFC) prefrontal cortex, the dorsal anterior cingulate/presupplementary motor cortex (dACC/preSMA) and the posterior parietal cortex have all been implicated in different aspects of working memory (Wager & Smith, 2003) and cognitive control (Niendam et al., 2012). Preparatory (e.g., cue or context-driven) task demands have primarily been associated with early, sustained DLPFC activity (Braver et al., 2009; Lesh et al., 2013). However, there is increasing evidence that other regions of the cognitive control network also function in proactive roles, dependent on task demands and individual differences in the utilization of proactive control. The dACC, for example, may proactively signal the need for control and is thought to recruit the implementation of cognitive control via other regions of the cognitive control network (Ide, Shenoy, Yu, & Li, 2013; Shenhav, Botvinick, & Cohen, 2013). In a stop signal task, the preSMA initially engages when preparing to stop, followed by right VLPFC activation, possibly implementing control (Swann et al., 2012). The striatum has also been implicated, with evidence that the anterior striatum (caudate and/or putamen) plays a role in activating a proactive inhibitory task set (Leunissen, Coxon, & Swinnen, 2016). Importantly, the extent that these mechanisms are utilized in a proactive fashion varies across individuals (Barch & Ceaser, 2012; Richmond, Redick, & Braver, 2015). Behavioral measures of proactive cognitive control are also correlated with working memory capacity and fluid intelligence (Kane & Engle, 2002; Redick, 2014; Redick & Engle, 2011), suggesting that they are more variably employed as a function of individual differences. Reactive cognitive control has traditionally been associated with engagement of the VLPFC and dACC/preSMA, as well as with more transient DLPFC activation (Braver et al., 2009; Irlbacher et al., 2014). VLPFC activation during reactive cognitive control tasks occurs during the inhibition of prepotent motor responses (Aron, Robbins, & Poldrack, 2014; Swick, Ashley, & Turken, 2011) and the resolution of the conflict between competing stimuli (D'Esposito, Postle, Jonides, & Smith, 1999). VLPFC activation has been found to be heavily implicated in reactive rather than proactive responding (Zandbelt, Bloemendaal, Hoogendam, Kahn, & Vink, 2013; Zandbelt, Bloemendaal, Neggers, Kahn, & Vink, 2013). Similarly, the dACC/preSMA is also associated with reactively detecting increases in error likelihood, sensory and/or response conflict (Botvinick, Cohen, & Carter, 2004; Carter & van Veen, 2007).

The current study used rapid data acquisition techniques, long cue–probe delays within the AX-CPT task (Paxton, Barch, Racine, & Braver, 2008; Paxton, Barch, Storandt, & Braver, 2006) and deconvolution to decouple the neural responses that occur during cue and probe phases of reactive and proactive cognitive control. Rather than assuming the shape of the hemodynamic response, deconvolution allows the shape of the hemodynamic response to vary. This approach permits more precise characterization of differences in both shape (e.g., prolonged activation) and delay that are known to vary across trials, regions, conditions/tasks, participants, and groups (Chen, Saad, Adleman, Leibenluft, & Cox, 2015; Lindquist, Meng, Atlas, & Wager, 2009). Although many tasks have been used to examine cognitive control (Derrfuss, Brass, Neumann, & von Cramon, 2005; Ridderinkhof, van den Wildenberg, Segalowitz, & Carter, 2004; Waskom, Kumaran, Gordon, Rissman, & Wagner, 2014), our hypothesese were primarily based on previous AX-CPT studies (Braver et al., 2009; Paxton et al., 2006; Paxton et al., 2008) given the ability to directly contrast both reactive ("AY" trials) and proactive processes (cues and "BX" trials) in the same experimental framework.

Based on these studies, we hypothesized that B relative to A cues would result in early, sustained activation of the DLPFC reflecting initiation of proactive cognitive control, triggering goal representations in advance of their implementation. We also hypothesized that proactive cognitive control would result in more variable behavioral and neural responses as a result of individual differences in utilization (Carter & van Veen, 2007; Lopez-Garcia et al., 2016; Richmond et al., 2015). Behavioral performance on BX trials is considered to be a primary measure of proactive control as faster reaction time indicates adequate preparation for the appearance of the probe (Barch et al., 2001; Dias et al., 2013). AY conditions, in contrast, are considered to require the greatest amount of reactive control as they are both minimally predicted by cues (12.5% of A cues are followed by Y probe) and require inhibition of a prepotent motor response. We predicted that probes with high reactive cognitive control demands (i.e., AY probes) would be associated with transient increased activation within the dACC/preSMA and VLPFC, and would exhibit a more homogeneous pattern of behavioral and neural responses across individuals.

2 | MATERIALS AND METHODS

2.1 | Participants

Fifty-two adult volunteers between the ages of 18–50 participated in the experiment. Two participants were excluded due to an inability to learn the task. No participant was identified as a motion outlier (more than three times the interquartile range on two of six framewise displacement parameters; Mayer, Franco, Ling, & Canive, 2007). Four participants were removed for poor behavioral performance during the task (accuracy below 68% on any single trial type, defined as chance based on a binomial distribution). There were no outliers on reaction time (RT) data on any measure.

Exclusion criteria consisted of (a) a history of severe neurological incidents or diagnoses (including head injury with greater than 30 min of loss of consciousness), (b) a developmental disorder (autism spectrum disorder or intellectual disability), (c) contraindications for MRI, (d) current pregnancy, (e) history of substance abuse/dependence or current use (confirmed with negative urine drug screen), (f) presence of any psychiatric disorder, (g) a first-degree relative with a psychotic spectrum disorder, or (h) a score of greater than 29 on the Beck Depression Inventory (BDI; Beck, Steer, & Brown, 1996). All participants provided informed consent according to institutional guidelines at the University of New Mexico Health Sciences Center.

2.2 | Clinical and neuropsychological assessments

The Measurement and Treatment Research to Improve Cognition in Schizophrenia Consensus Battery (MCCB; Kern et al., 2008; Nuechterlein et al., 2008) was used as an independent and validated measure of neuropsychological functioning. A vigilance factor was derived from a continuous performance test whereas a planning factor was

derived from the Mazes subtest. Finally, a working memory factor was collectively derived from the Wechsler Memory Scale III Spatial Span and Letter Number Span. Domain t-scores were obtained based on normative data for all factors (Kern et al., 2008; Nuechterlein et al., 2008).

2.3 | Task description

All participants completed an AX-CPT task (Figure 1a,b) in which they monitored a continuous series of visual cues (the letters A, R, V, P, S, and E; duration = 500 ms) and auditory probes (the letters X, Q, F, I, M, and U; duration = 500 ms). A visual cue was used with an auditory probe as previous studies indicate this combination results in maximum crossmodal cueing effects (Yang & Mayer, 2014). Non-"A" (hereafter referred to as B cues) and non-"X" (hereafter referred to as Y probes) letters were selected to be visually or aurally distinct from their respective counterparts. Participants pressed a button with either their right index ("yes" response) or middle ("no" response) finger following the presentation of each cue and each probe. Button presses were logged between 100 and 2000 ms following stimuli to exclude anticipatory or late responses, respectively. The inter-stimulus interval (2,760–3,680 ms) and inter-block interval (4,060–4,980 ms) were jittered with a minimum delay of approximately 2.7 s to minimize nonlinear summing of the hemodynamic response function (HRF) between the cue and probe phases and to decrease temporal

expectations (Glover, 1999). The resulting design matrix was mathematically well-conditioned and invertible with only moderate collinearity among the various behavioral regressors.

The cue letter A occurred on 80% of total trials. The target sequence consisted of an A cue followed by an X probe, and this AX cue/probe sequence occurred on 70% of the total trials. Participants indicated the appearance of the target sequence with a "yes" response following the probe. Participants responded to all cues (the letters A, R, V, P, S, and E) and all other probes (the letters Q, F, I, M, and U) with a "no" response. AY sequence trials (10% frequency) occurred when an A cue was followed by a Y probe. The AY sequence theoretically results in both a violation of expectation and the inhibition of a prepotent motor response due to the preponderance of AX sequences (which sets one up to expect an X following an A), and thereby maximizes the demand for reactive cognitive control (Cohen, Barch, Carter, & Servan-Schreiber, 1999).

In contrast, participants theoretically always know to make a "no" response to any probe that follows the presentation of a B cue, which should maximally engage proactive cognitive control relative to AX and AY trials. Specifically, while participants must still inhibit a prepotent motor response following a BX sequence (10% frequency), the proactive utilization of information from the B cue should prepare them to make a "no" response (Cohen et al., 1999). BY sequence trials (10% frequency) were included to generate the expected cognitive set
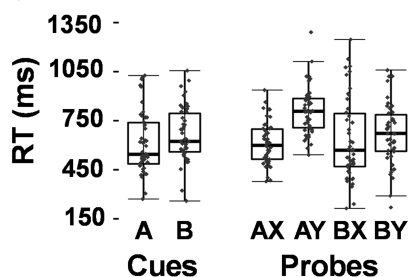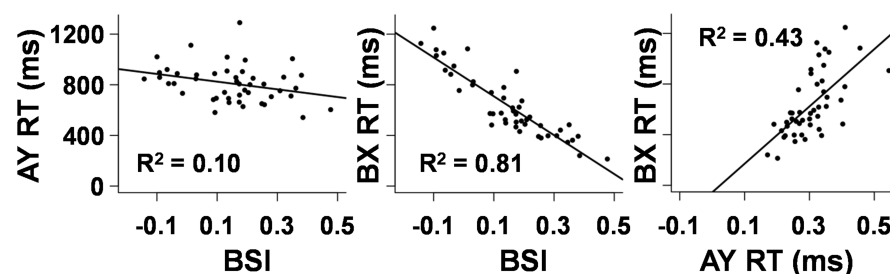

(a) Task Design A Conditions
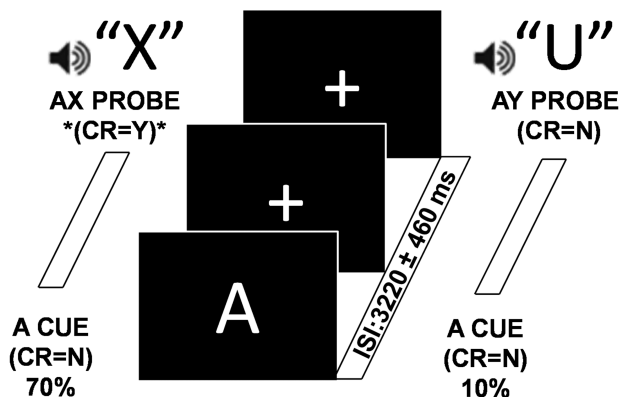
(b) Task Design B Conditions
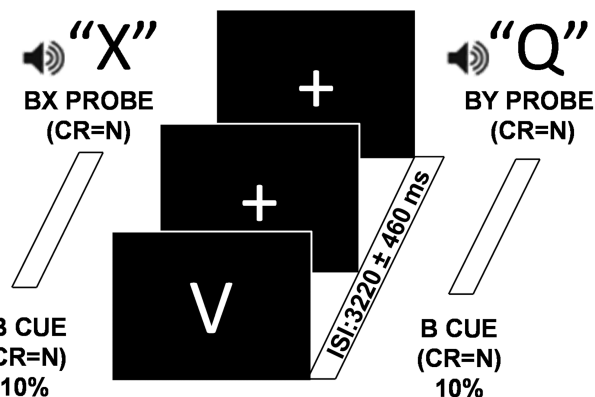
(c) Reaction Time

(d) Proactive Cognitive Control Measures

FIGURE 1 Diagrammatic representation of task and behavioral results. The required correct response (CR) was "yes" (Y) when the letter X followed the letter A (target sequence AX; denoted with an asterisk; 70% of trials; panel a left). The three remaining conditions (AY, panel a right; BX and BY, panel b) all require a "no" (N) response to both cue and probe and each occurred on 10% of trials. The inter-stimulus interval (ISI) was 3,220 ms jittered by one TR (2760–3,680 ms). The inter-block interval was 4,520 ms and also jittered by one TR (4060–4,980 ms). Box-and-whisker plots depict reaction times (RT) for all task conditions (panel c). Scatter plots (panel d) depict the relationships between behavioral measures of proactive and reactive cognitive control (BSI = behavioral shift index, AY RT, and BX RT)

based on cue/probe probabilities used in previous studies but were not of primary interest in data analyses. Letter sequences were presented in a pseudorandom order, but always maintained the same probability structure within each run (i.e., AX = 70%; AY = 10%; BY = 10%; BX = 10%), resulting in the following trial counts: AX = 112; AY = 16; BX = 16; BY = 16. Participants received instructions and completed practice (until performance indicated understanding of task) prior to entering the scanner.

2.4 | Behavioral analyses

Accuracy (percent correct), median RT for correct trial data and response variability were computed for cues (A, B) and all of the probe trial types (AX, AY, BX, and BY). Within-subjects *t* tests examined RT differences across the following contrasts: A versus B cues; AX versus AY probes; AX versus BX probes; and AY versus BX probes. Wilcoxon signed-rank tests examined nonnormally distributed accuracy data. Finally, Pitman tests were chosen to examine within subject response variability across conditions. Specifically, a correlation coefficient was computed between the sum (e.g., Probe X + Probe Y) and difference (e.g., Probe X – Probe Y) between two conditions and assessed for significance (Piepho, 1997).

A series of three multiple regressions were conducted using separate behavioral metrics from the AX-CPT task (behavioral shift index [BSI], AY, and BX RTs) as the dependent variable and MCCB factors (vigilance, working memory, and planning) as the independent variables. The BSI represents the most typically used metric from the AX-CPT task (Paxton et al., 2006, 2008) for determining whether the individual is responding in a highly proactive (i.e., large positive index score) or reactive (i.e., small or negative index) manner. The BSI was computed using RT as follows:

$$BSI = \frac{AY - BX}{AY + BX}$$

2.5 | Imaging, processing, and statistical analyses

High resolution 5-echo multi-echo Magnetization Prepared Rapid Acquisition Gradient High resolution 5-echo multi-echo Magnetization Prepared Rapid Acquisition Gradient Echo (MPRAGE) T_1 [repetition time (TR) = 2,530 ms; echo times (TE) = 1.64, 3.5, 5.36, 7.22, and 9.08 ms; inversion time (TI) = 1,200 ms; flip angle = 7; number of excitations (NEX) = 1; slice thickness = 1 mm; field of view (FOV) = 256 mm; matrix size = 256 × 256; isotropic voxels = 1 mm] were collected for structural images on a 3T Siemens Trio Tim scanner.

Echo-planar images were collected for four runs of the AX-CPT task using a single-shot, gradient-echo echoplanar pulse sequence with simultaneous multi-slice technology (TR = 460 ms; TE = 29 ms; flip angle = 44°; multiband acceleration factor = 8; NEX = 1; slice thickness = 3 mm; FOV = 248 mm; matrix size = 82 × 82; 56 interleaved slices; 3.02 × 3.02 × 3.00 mm voxels). The first three images of each run were eliminated to account for T_1 equilibrium effects, resulting in a total of 3,116 images for the final analysis. A single band reference image (SBREF) was also acquired to facilitate registration with the T_1 image. Two EPI distortion mapping prescan sequences (TR = 7,220 ms; TE = 73 ms; flip angle = 90°; refocus flip angle = 180°; slice thickness = 3 mm; FOV = 248 mm; matrix size = 82 × 82; 56 interleaved slices; 3.02 × 3.02 × 3.00 mm voxels) with reversed phase encoding directions (A → P; P → A) were also collected to correct for susceptibility related artifacts in the task data.

Anomalous time-series data were first identified and replaced based on values from the previous and subsequent image using AFNI's despiking protocol (Cox, 1996). All time-series data were then temporally interpolated to the first slice to account for differences in slice acquisition and spatially registered in two- and three-dimensional space to the SBREF to reduce the effects of head motion. Susceptibility-induced field distortion was estimated and corrected using FSL Topup (Andersson, Skare, & Ashburner, 2003; Smith et al., 2004). Task data were converted to standard stereotaxic coordinate space (Talairach & Tournoux, 1988) using a nonlinear algorithm (AFNI 3dQwarp) and spatially blurred using a 6-mm Gaussian full-width half-maximum filter. A voxel-wise deconvolution analysis generated a single HRF for each trial-type based on the first 14.26 s post-stimulus onset relative to the baseline state (visual fixation plus gradient noise). In contrast to typical analyses, this approach allows for the shape of the HRF to vary, allowing for examination of not only the amplitude of the HRF but also prolonged activation. Error trials were modeled separately for each trial type to eliminate error variance (Mayer et al., 2011).

As our a priori hypotheses posited sustained DLPFC activity, two separate percent signal change (PSC) windows were calculated by summing the beta coefficients for images occurring between 3.22 and 5.06 s (peak activation) and between 5.06 and 6.90 s (late peak) post-stimulus onset and dividing by the average model intercept. These time windows were selected to maximize similarities in HRFs across motor, sensory, and prefrontal cortex. Importantly, this procedure was done prior to any analyses and based on averaged data (i.e., all participants averaged across all trials) to avoid any potential bias. A 2 × 2 [Cue (A vs. B) × Time (Peak Activation vs. Late Peak)] repeated-measures ANOVA was conducted to examine functional activation across cue types. A similar 2 × 2 analytic strategy was utilized to examine the difference among probes (AX vs. AY, AX vs. BX, and AY vs. BX).

"Sustained" activation was operationally defined as regions exhibiting significant Condition × Time interactions in which the difference was being driven by differential activity in the late peak phase. The main effects of Time were not of interest to current analyses. Following standard statistical conventions, only the interaction terms were evaluated for any regions exhibiting both a significant effect of Condition and a Condition × Time interaction. All voxel-wise results were corrected for false positives at *p* < .05 based on 10,000 Monte-Carlo simulations (*p* < .001 and minimum cluster size = 602 μl) using the spherical autocorrelation estimate in AFNI.

3 | RESULTS

The final cohort included 46 participants (28 males; mean age = 31.8 ± 7.4 years; mean education = 15.2 ± 1.9 years). Forty-five of the participants reported negligible (depression score 0–13), no

participant reported mild (depression score 14–19), and one participant reported moderate depression (20–28).

3.1 | Behavioral analyses

Results indicated that participants exhibited significantly ($t_{45} = -4.68$, $p < .001$) faster RT for A (611.44 ± 187.16 ms) relative to B (664.44 ± 167.85 ms; Figure 1c) cues in conjunction with a trend for decreased variability in B relative to A cues (Pitman test $r = 0.26$; $p = .084$). In contrast, there were no differences in accuracy data for A (97.43 ± 3.80%) and B (96.58 ± 5.60%) cues. RTs (Figure 1c) for AY probes (809.64 ± 145.11 ms) were significantly slower than to both AX (610.58 ± 129.67 ms; $t_{45} = -16.17$, $p < .001$) and BX (633.76 ± 251.84 ms; $t_{45} = -6.21$, $p < .001$) probes. There were no significant differences in RT between AX and BX probes. RT variance was significantly greater for BX relative to both AX ($r = -.71$; $p < .001$) and AY ($r = -.61$; $p < .001$) probes, with similar amounts of variance observed for AX and AY probes ($p > .10$) in spite of differences in RT. Finally, accuracy for BX probes (93.23 ± 7.83%) was significantly lower than both AX (96.57 ± 4.64%; $Z = -2.57$, $p = .01$) and AY probes (96.45 ± 5.39%; $Z = -2.62$, $p = .01$). BY RT (675.64 ± 192.76 ms) and accuracy (98.50 ± 3.29%) were not explicitly analyzed as part of a priori comparisons, but are included for thoroughness.

Secondary analyses were also conducted to examine the relationship between the BSI and the individual RT scores (BX = proactive cognitive control; AY = reactive cognitive control). Results (Figure 1d) indicted a strong inverse correlation between the BSI and BX RT ($r = -.90$; 81.0% of total variance; $p < .001$), with a weaker relationship present between BSI and the AY RT ($r = -.31$; 9.5% of total variance; $p = .04$).

Secondary regression analyses indicated significant relationships between the working memory score and both the BSI RT ($\beta = 0.44$, $t_{42} = 2.70$, $p = .01$) and BX RT ($\beta = -0.37$, $t_{42} = -2.19$, $p = .03$). Results from the AY RT (reactive cognitive control measure), planning and vigilance variables were not significant. Exploratory correlation analyses were conducted between the MCCB measures and median RT for the remaining cues and probes given the negative results with vigilance and planning measures. The working memory factor was significantly inversely correlated with RT on the A and B cues (all p's < .05). In contrast, the vigilance and planning measures were not related to RT data from either cues or probes (all p's > .10).

3.2 | Functional task results: cue-related activity

Results from all functional analyses are summarized in Supporting Information Table S1. To ensure the results were not affected by symptoms of depression, we ran additional analyses that included the BDI score as a covariate. All reported clusters survived when BDI was used as a covariate in functional analyses. A 2 × 2 [Condition (A vs. B cue) × Time (Peak Activation vs. Late Peak)] repeated-measures ANOVA was used to test our a priori hypotheses regarding the utilization of proactive cognitive control following the presentation of B relative to A cues across the peak and late peak phases. Results indicated increased activation in the right VLPFC extending into the anterior insula (aI/VLPFC; BAs 13/44/45; μl = 751) for B relative to A cues
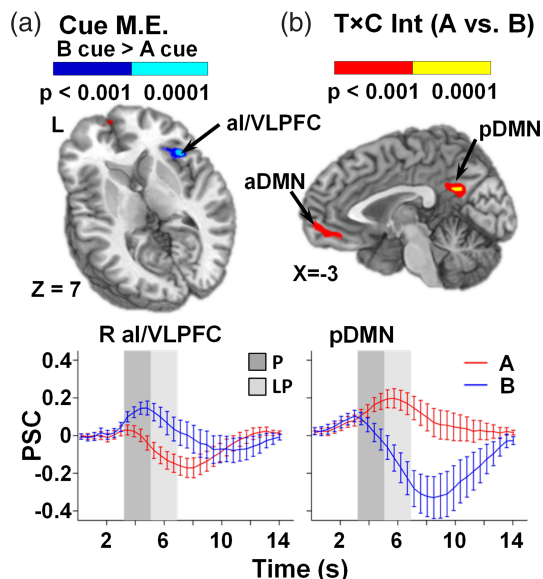

FIGURE 2 Panel a presents regions exhibiting a main effect (M.E.) for cues, with greater activation ($p < .001$: blue; $p < .0001$: cyan) for B relative to A cue trials in the right anterior insular/ventrolateral prefrontal cortex (aI/VLPFC; Center of Mass: 40.5, 16.2, and 5.7). Panel b presents regions exhibiting a significant interaction between time (T) and condition (C) for A and B cue trials ($p < .001$: red; $p < .0001$: yellow) in the bilateral anterior (aDMN; Center of Mass: −0.4, 46.3, and 0.4) and posterior default mode network (pDMN; Center of Mass: 0.8, −52.3, and 25.5). Locations of sagittal (X) and axial (Z) slices are given according to the Talairach atlas for the left (L) hemisphere. Percent signal change (PSC) extracted across each region are plotted over the entire hemodynamic response function (HRF) for A (red) and B (blue) cue conditions, with error bars reflecting the standard error across participants. Shaded bars indicate peak (P; dark gray) and late peak (LP; light gray) phase of HRF

(Figure 2a). There was a significant Condition × Time interaction in the bilateral ACC and medial frontal gyrus (anterior default mode network [DMN]; BAs 10/24/32; μl = 3,230) and the posterior cingulate/precuneus (posterior DMN; BAs 23/31; μl = 1,043; Figure 2b). Simple effects tests indicated greater activation in DMN regions in response to A cues relative to deactivation following B cues during the late peak compared to peak phase.

3.3 | Functional task results: probe-related activity

A similar series of 2 × 2 ANOVAS were used to test our a priori hypotheses about differential activation for reactive cognitive control (AY probes) and proactive cognitive control (BX probes) probe trials across the peak and late peak phases. The first analyses compared AY versus AX probes, with a main effect of Probe (AY > AX for both peak and late peak phases) observed within the thalamus (μl = 10,119) and left caudate (μl = 1,062). Significant interactions indicated sustained activation (i.e., greater AY relative to AX activation in late peak phase only) within the right (BAs 9/10; μl = 1801) and left (BAs 10/46; μl = 2,989) superior frontal gyrus/DLPFC, bilateral precuneus (BA 7; μl = 3,432), left claustrum/putamen (BAs 13; μl = 602), and right (μl = 10,165) and left (μl = 10,527) cognitive regions (i.e., lobule VIIa Crus I and II) of the cerebellum (Figure 3). There was also a larger difference in the magnitude of activation
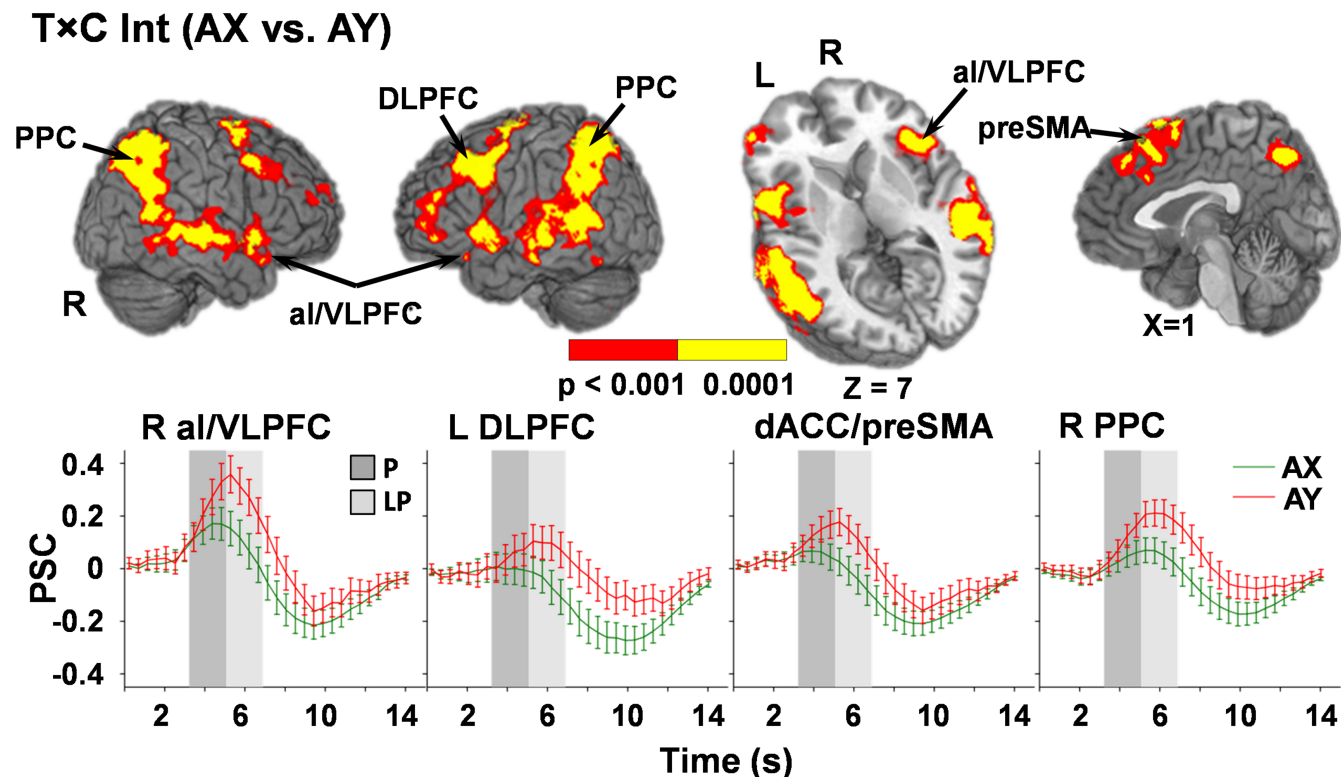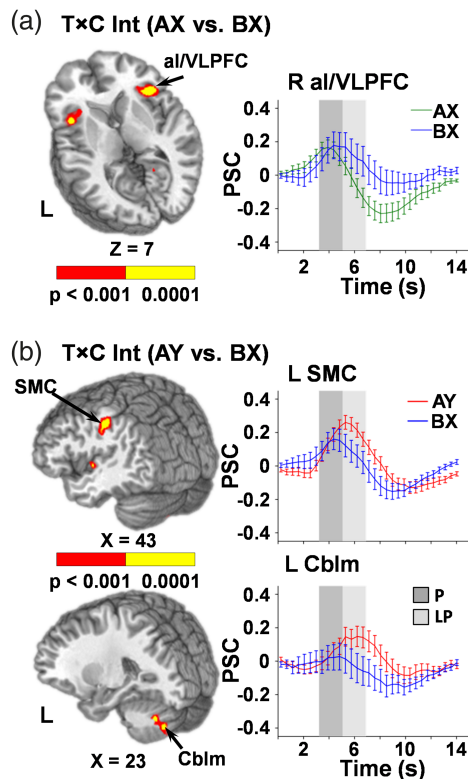
FIGURE 3 Regions exhibiting a significant interaction between time (T) and condition (C) for AX relative to AY trials ($p < .001$: red; $p < .0001$: yellow). Locations of the sagittal (X) and axial (Z) slices are given according to the Talairach atlas for the left (L) and right (R) hemispheres. Percent signal change (PSC) extracted across each region are plotted over the entire hemodynamic response function (HRF) for AY (red) and AX (green) probe conditions, with error bars reflecting the standard error across participants. Shaded bars indicate peak (P; dark gray) and late peak (LP; light gray) phases of HRF. Selected regions include left and right posterior parietal cortex (PPC; Center of Mass: left, −41.3, −54.7, 40.9; right, 42.8, −58.8, 39.8), anterior insular/ventrolateral prefrontal cortex (aI/VLPFC; Center of Mass: left, −46.8, 8.0, 0.8; right, 47.9, 14.1, −1.8), dorsolateral prefrontal cortex (DLPFC; Center of Mass: left, −45.3, 10.9, 35.9; right, 42.2, 14.1, 39.2), dorsal anterior cingulate cortex/pre-supplementary motor cortex (dACC/preSMA; Center of Mass: 2.1, 20.4, 47.7)

during the late peak compared to the peak phase (sustained activation; AY > AX) within the right (BAs 6/8/9; μl = 6,124) and left (BAs 6/8/9/44/45; μl = 10,279) premotor/frontal eye fields/DLPFC, bilateral dACC/preSMA (BAs 6/8/32; μl = 4,997), right (BAs 13/22/38/44/45/47; μl = 8,168) and left (BAs 13/22/38/44/45/47; μl = 9,087) aI/VLPFC, right (BAs 7/19/39/40; μl = 12,369) and left (BAs 7/19/39/40; μl = 13,559) posterior parietal cortex, and the right (BAs 21/22; μl = 17,748) and left (BAs 13/21/22/39/40/41/42; μl = 19,058) primary and secondary auditory cortices extending into the inferior, middle, and superior temporal gyrus.

Results of the 2×2 repeated-measures ANOVA examining (AX and BX) probes indicated significant interactions in five different clusters. Simple effects testing of the interaction indicated sustained activation for the right (BAs 13/44/45/47, μl = 2,038) and left (BAs 13/45/47, μl = 1,213) aI/VLPFC for the BX relative to AX probes during the peak phase (Figure 4a). In contrast, the right posterior aspect of the middle temporal gyrus (BAs 19/39; μl = 791) demonstrated greater activation for BX relative to AX probes during the peak phase only (suggesting brief, rather than sustained activation). Finally, although significant interactions were observed in the right precuneus/posterior cingulate gyrus (BAs 29/30/31; μl = 789) and secondary auditory cortex/middle temporal gyrus (BAs 21/22 μl = 915), follow-up simple effects tests were negative.

The ANOVA examining reactive control processes (AY relative to BX probes) indicated significant interactions within the left sensorimotor cortex extending into inferior parietal lobe (BAs 2/40/42/43, μl = 2,628), right lobule VIIIa of the cerebellum (motor region; μl = 757) and left lobule VIIa Crus I and II of the cerebellum (cognitive regions; μl = 849; Figure 4b). Simple effects tests indicated that the interaction in these areas resulted from sustained activation during the AY relative to BX trails. A significant interaction was also present within the secondary auditory cortex (BAs 6/13/22; μl = 797); however, testing of all simple effects within this cluster was not significant.

A series of three follow-up regression analyses were conducted to determine if differences in functional activation during cues (i.e., calculated A − B PSC for regions in Figure 2) or behavioral metrics (i.e., AY, BX) were associated with differences in functional activation (i.e., calculated AY − BX PSC for regions in Figure 4b) during the late peak phase of probes. The BSI was excluded due to evidence of strong multicollinearity with its RT components. Results indicated the difference in activation within the right aI/VLPFC during cues (A−B) was significantly and inversely related to the difference in activation during probes (AY−BX) in the sensorimotor cortex ($\beta = -0.58$, $t_{40} = -4.59$, $p < .001$), left lobule VIIa Crus I and II of the cerebellum ($\beta = -0.47$, $t_{40} = -3.85$, $p < .001$), and right lobule VIIIa of the cerebellum ($\beta = -0.58$, $t_{40} = -4.96$, $p < .001$; Figure 5). In addition,

FIGURE 4 Regions exhibiting a significant interaction between time (T) and condition (C) for AX relative to BX trials (panel a) and AY relative to BX trials (panel b; $p < .001$: red; $p < .0001$: yellow). Locations of the sagittal (X) and axial (Z) slices are given according to the Talairach atlas for the left (L) and right (R) hemispheres. Percent signal change (PSC) extracted across each region are plotted over the entire hemodynamic response function (HRF) for AX (green), BX (blue), and AY (red) conditions, with error bars reflecting the standard error across participants. Shaded bars indicate peak (P; dark gray) and late peak (LP; light gray) phase of the HRF. Selected regions include bilateral anterior insula/ventrolateral prefrontal cortex (aI/VLPFC; Center of Mass: 40.4, 19.2, 4.7) for the AX relative to BX contrast and the left sensorimotor cortex (SMC; Center of Mass: 47.3, −24.6, 33.8) and the left cerebellum (Cblm; Center of Mass: −23.2, −67.1, −35.2) for the AY relative to BX contrast

activation in the DMN (averaged across both regions) was significantly related to the difference in activation during probes in the left ($\beta = -0.31$, $t_{40} = -2.55$, $p = .02$) and right ($\beta = -0.25$, $t_{40} = -2.14$, $p = .04$) lobules of the cerebellum (Figure 5). The three behavioral indices were not associated with differential activation on AY versus BX probes (all p's > 0.10).

3.4 | Secondary analyses: baseline contrasts and variability analyses

Our principal analyses did not support a priori predictions of increased DLPFC activity for B relative to A cues or during BX probes. Secondary analyses were therefore performed to examine cue and probe activation relative to baseline state during the peak phase. In addition to the regions found to significantly differ between cues during direct comparisons (i.e., right aI/VLPFC and the anterior/posterior nodes of the DMN), the bilateral DLPFC (BAs L = 9/46, BAs R = 9) demonstrated significant activation during B cues relative to baseline, which

was absent during A cues (Figure 6a). Results also indicated common activation across both cue conditions in the bilateral preSMA/SMA/premotor cortex (BA 6), visual cortices (BAs 18/19/37), posterior cingulate (BAs 23/31), lobule VI of the cerebellum and left sensorimotor cortex (BAs 2/3/4).

Both probes following A cues (AX and AY trials) elicited widespread activation relative to baseline in the bilateral pre-SMA/SMA/premotor cortex (BA 6), DLPFC (BAs 9/10), aI/VLPFC (BA 13/44), auditory cortices extending into the temporal lobe (BAs 22/40/41/42), thalamus, lobule VI and lobule VIIIa of the cerebellum, and left sensorimotor cortex (BAs 2/3/4) during the peak phase (Figure 6b). In contrast, probes following B cues (BX and BY trials) elicited relatively sparse activation relative to the baseline state, with activity limited to the bilateral auditory cortex extending into the temporal lobe and insula (BAs 13/21/22/41/42). BX probes showed additional activation within the left sensorimotor cortex (BAs 3/4; Figure 6c).

Region of interest-based Pitman Tests were then conducted to examine if HRF variability across participants partially explained the null findings versus baseline in the BX probes relative to the large degree of activation observed following AY probes (see larger error bars in Figures 2–4). These analyses focused on left primary motor cortex (PMC; 12 mm diameter sphere around Talaraich coordinates −39, −38, and 54) and supplementary motor area (SMA; −2, −7, and 55) based on the assumption that participants at a minimum had to press a button to ensure a correct response for both BX and AY trials. Results indicated increased variability for BX relative to AY probes during both the peak and late peak phases within the PMC (r's = −.55 and −.60, respectively) and SMA (r's = −.65 and −.66; all p's < .01; Figure 6d). These analyses were extended to the pre-peak HRF (1.38–3.22 s) phase, with results again indicating that variability was greater for BX relative to AY probes in both motor regions (PMC $r = -.53$; SMA $r = -.69$) during this early window (all p's < .01; Figure 6d).

Pitman tests were therefore also conducted to determine whether HRF variability was greater within the PMC and SMA during the peak, late peak, and an after peak phase (encompassing 6.90–8.30 s) following cues (Figure 6e). There were no differences between A and B cues in the peak and late peak phases for either motor region. However, significantly greater variability was observed within both the PMC ($p = .014$; $r = -.36$) and SMA ($p = .008$; $r = -.38$) during the after peak phase for B relative to A cues.

Given our null results, supplemental region of interest analyses were conducted to examine peak and late peak PSC within the DLPFC (6 mm radius spheres around: right −41, 18, 28 and left 41, 18, 28) using identical statistical approaches. Results indicated no significant differences in left and right DLPFC activity during A versus B cue, AX versus BX probe and AY versus BX probe comparisons. Consistent with whole-brain results, there were significant interactions for the AX and AY conditions in the left ($F_{1,45} = 16.64$, $p < .001$) and right ($F_{1,45} = 20.32$, $p < .001$) DLPFC, with simple effects testing indicating increased activation during the late peak compared to the peak phase (sustained activation; AY > AX) across the left and right DLPFC. There was a main effect ($F_{1,45} = 38.06$, $p < .001$) of probe in the left DLPFC only.
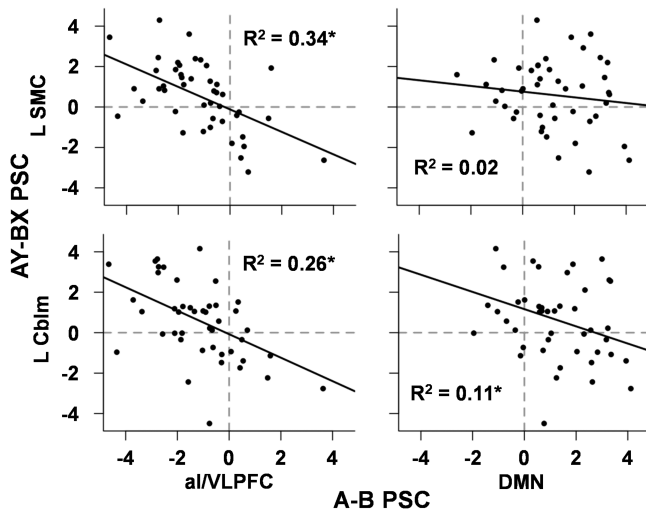
FIGURE 5 Scatter plots depicting relationships between regions showing significant differences in cue (A, B) and subsequent probe (AY–BX) related activity. Results indicated significant inverse relationships between differential cue-related activation in anterior insula/ventrolateral prefrontal cortex (aI/VLPFC) and differential probe-related activation in the left sensorimotor cortex (L SMC), right (not pictured) and left cerebellum (L Cblm). Specifically, greater differences in right aI/VLPFC during cues were associated with greater differences between AY and BX probe responses, most likely as a result of neural suppression during BX trials. In contrast, a significant inverse relationship was found between differential cue-related activation in the default mode network (DMN) and only the L Cblm. Asterisks denote significant relationships

4 | DISCUSSION

In the current study, measures of proactive cognitive control resulted in activation of the right aI/VLPFC during the cue period (B relative to A cues) and activation of the bilateral aI/VLPFC during the probe period (BX vs. AX). High levels of both behavioral and neural variability characterized proactive cognitive control, suggesting large individual differences in actual implementation. Reactive cognitive control, in contrast, elicited a more homogeneous pattern of behavioral and neural responses across individuals. Specifically, AY relative to AX probes resulted in increased RTs and neural activation within the bilateral dACC/pre-SMA, DLPFC, aI/VLPFC, and posterior parietal cortex. Considered collectively, these results highlight a common and potentially flexible role of the aI/VLPFC for instantiating both proactive and reactive cognitive control across multiple phases of the AX-CPT task.

Behavioral results from our intermodal paradigm (visual cues with auditory targets) were consistent with previous AX-CPT studies that utilized visual stimuli only (Barch et al., 2001; Barch, Carter, MacDonald III, Braver, & Cohen, 2003; Braver et al., 2009; Paxton et al., 2006; Paxton et al., 2008), suggesting that proactive and reactive cognitive control function in a supramodal fashion. RTs were slower for B relative to A cues and for AY relative to AX and BX probes, consistent with designs with longer (Braver et al., 2009; Paxton et al., 2008) rather than shorter (Barch et al., 2001; Poppe et al., 2016) cue–probe delays. BX probes were associated with both decreased accuracy and increased RT variability, which subsequently captured the majority of BSI variance relative to AY trials. Although the latter finding was likely

driven by the increased range of RT during BX trials, it suggests that direct comparisons of AY and BX trials represent a more parsimonious approach for characterizing reactive versus proactive cognitive control rather than the BSI.

The 100% predictive nature of B relative to A cues has been suggested to proportionally increase the degree of DLPFC engagement triggering goal representations in advance (Blackman et al., 2016; Braver, 2012; Braver et al., 2009). However, in the current experiment B cues resulted in activation of right aI/VLPFC rather than the DLPFC, as well as deactivation of the DMN. The aI/VLPFC has classically been associated with reactive response inhibition (Aron et al., 2014; Cieslik, Mueller, Eickhoff, Langner, & Eickhoff, 2015; Rae, Hughes, Weaver, Anderson, & Rowe, 2014; Swick et al., 2011). Divergent viewpoints exist regarding whether VLPFC activation following a cue reflects proactive activity in the response inhibition network (i.e., proactive preparation; Aron, 2011; Zandbelt, Bloemendaal, Neggers, et al., 2013) or violations in expectation (Zandbelt, Bloemendaal, Neggers, et al., 2013). As both patterns could contribute to the observed activation during the presentation of infrequent B cues, future studies are needed to more carefully and directly dissociate potential differences between proactive preparation and violation of expectation that occurs following B cues in the AX-CPT task.

Additionally, we observed DMN deactivation during the proactive cue condition in conjunction with the anterior insula and VLPFC activation. DMN deactivation, often referred to as suppression, reliably occurs when tasks require increased cognitive load and externalized attention (Buckner, Andrews-Hanna, & Schacter, 2008; Gusnard & Raichle, 2001). As the DMN plays a key role in mind-wandering and internally mediated cognitive processes, the DMN deactivation is thought to reflect a decrease in these irrelevant cognitive functions in the face of tasks that require increased cognitive control (Anticevic et al., 2012). There are dynamic interactions between the cognitive control network and the DMN, processes thought to be mediated by the right frontoinsular cortex (Menon & Uddin, 2010; Sridharan, Levitin, & Menon, 2008). As proactively responding to B cues triggers engagement of proactive control processes, the observed activation of the anterior insula and deactivation of the DMN may reflect a proactive switch in network engagement and/or external attention capture due to increased salience of infrequent events.

The lack of DLPFC activity during both cue and probe proactive cognitive control conditions in the current study is notable (Braver, 2012) and may be the result of several factors. First, proactive cognitive control has been operationally defined in several different ways, even within the AX-CPT task. For example, previous studies (Braver et al., 2009; Paxton et al., 2006, 2008) have compared cues (A + B; proactive) to probes (AY + BX; reactive). However, current results suggest very different patterns of activity across AY versus BX probes, which would necessarily skew resultant contrasts toward the more active AY condition. Second, behavioral results indicated that similar relationships existed between both A and B cue RT with an independent measure of working memory, suggesting that both cues utilized proactive cognitive control to some degree. Finally, variations in task design (e.g., longer inter-stimulus intervals, differences in the frequency of BX probes) also influence how participants utilize cue
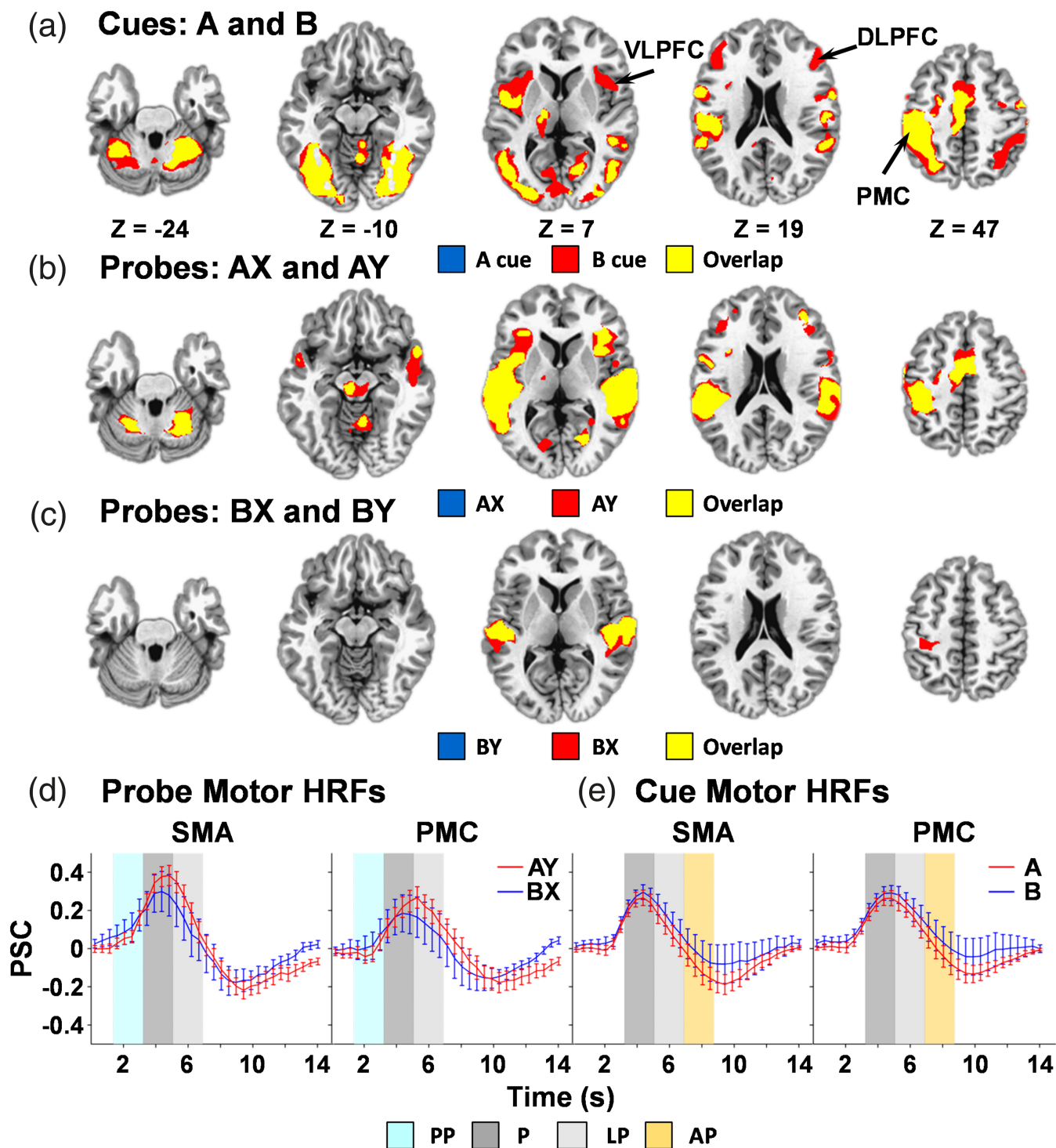
FIGURE 6 Overlay plots depicting activation for cue conditions (panel a), a probe conditions (AX and AY, panel b), B probe conditions (BX and BY, panel c) relative to baseline. Highlighted regions include anterior insula/ventrolateral prefrontal cortex (VLPFC), dorsolateral prefrontal cortex (DLPFC), and primary motor cortex (PMC). Locations of the axial (Z) slices are given according to the Talairach atlas for the left (L) and right (R) hemispheres. Percent signal change (PSC) data are plotted over the entire hemodynamic response function (HRF) for the supplementary motor area (SMA) and PMC regions of interest for probes (panel d) and cues (panel e), with error bars reflecting the standard error across participants. Shaded regions of the HRF indicate pre-peak (PP; cyan), peak (P; dark gray), late peak (LP; light gray), and after-peak (AP; orange) phases

information (Lesh et al., 2013; Lopez-Garcia et al., 2016) and may ultimately alter DLPFC recruitment.

Additionally, while the current study did not aim to differentiate the role of the striatum in proactive and reactive control, it is notable that we did not observe differential effects following the presentation of a proactive relative to a reactive cue (Leunissen et al., 2016;

Zandbelt, Bloemendaal, Neggers, et al., 2013). The striatum activates a proactive inhibitory task set in preparation for subsequent trials during proactive inhibition (Zandbelt & Vink, 2010). However, the striatum is also robustly involved in reactive control (Aron, Behrens, Smith, Frank, & Poldrack, 2007; Coxon, Stinear, & Byblow, 2006; van den Wildenberg et al., 2010). Previous investigations rely on the stop

signal task which manipulates the probability of a stop signal to capture the magnitude of response slowing as an index of "proactive inhibition" (Aron, Behrens, Smith, Frank, & Poldrack, 2007; Chikazoe et al., 2009; Zandbelt & Vink, 2010). The proactive inhibition required by this task, however, provides 100% required information to definitely switch the response selection. These divergent task designs likely account for the lack of striatal involvement in the current study.

Probe-related reactive cognitive control (AY > AX) resulted in widespread activity of the classical cognitive control network including bilateral DLPFC (extending into the inferior frontal junction; Brass, Derrfuss, Forstmann, & von Cramon, 2005), VLPFC, dACC/pre-SMA, and posterior parietal cortex. In contrast, probe-related proactive cognitive control (BX > AX) resulted in isolated activity within the bilateral aI/VLPFC, the same region identified during both B vs. A cue comparisons and during reactive cognitive control (compare Figures 2–4). The bilateral aI/VLPFC activation across both types of probe trials likely results from a common requirement to reactively inhibit prepotent responses due to violations in expectations (AY trials) or from the appearance of a habitual stimulus (BX trials). Surprisingly, the direct comparison of AY vs. BX probes resulted in increased activation (AY > BX) in the left sensorimotor cortex/inferior parietal lobe, right motor and left cognitive regions of the cerebellum (Buckner, 2013) rather than within the traditional cognitive control network. The differential activity in motor circuitry between AY and BX probes was unexpected given that both trials minimally required a button press to indicate a correct trial.

Examination of the neural activation highlighted that proactive conditions demonstrated significantly greater variability relative to reactive conditions. Specifically, an increase in HRF variability began after the late peak phase (encompassing 6.90–8.30 s postcue onset) of B cues. The increased variability was also observed in motor circuitry (PMC and SMA) during the pre-peak (encompassing 1.38–3.22 s post probe onset), peak, and late peak phases of the HRF during BX relative to AY probes. Although quantitative analyses focused on motor circuitry, qualitative examinations of HRF (Figures 2–4) suggest that increased variability was robustly present across all brain regions following B cues and subsequent probes. This pattern highlights that conditions allowing for the utilization of proactive control demonstrate greater variability than those associated with reactive control (which are also largely reliant on reactive stopping). This is consistent with previous work that suggests outright stopping results in consistent neural responses, regardless of strategy, whereas neural activation patterns associated with attention-related processes varied based on strategies utilized by the individual (Sebastian et al., 2017). A further result of this neural variability was the relatively sparse activation (common activation of auditory cortex only) for B probes (BX and BY) relative to the baseline state in comparison to robust activation of prefrontal (aI/VLPFC, DLPFC, and dACC/pre-SMA), motor, auditory, and posterior parietal cortex relative to baseline during both A probes. In other words, the increased individual variability contributed to the null findings when examined in group-level analyses. These results highlight that studying attention and cognitive control-related processes should incorporate an examination of strategic differences.

Finally, regression analyses demonstrated that neural variability observed during AY vs. BX comparisons (left sensorimotor cortex, right and left cerebellum) was associated with cue-related activity in the aI/VLPFC. Specifically, individuals who exhibited stronger aI/VLPFC activation for B cues also exhibited weaker BX neural responses within motor circuitry (i.e., most data localized to upper right quadrants in Figure 5). Thus, these findings provide preliminary evidence that the aI/VLPFC proactively modulates or potentially suppresses subsequent neural activity (motor programs) during B probe periods in some individuals (Aron, 2011; Chikazoe et al., 2009; Jahfari, Stinear, Claffey, Verbruggen, & Aron, 2010), leading to a high degree of variability in neural responses when the group is examined as a whole. However, there is increasing evidence that the aI and VLPFC are functionally heterogeneous and may play differential roles in detecting behaviorally salient events or implementing inhibitory control, both of which may occur in a proactive or reactive fashion (Bartoli, Aron, & Tandon, 2018; Cai, Ryali, Chen, Li, & Menon, 2014). Similar to previous results, behavioral metrics of proactive cognitive control were related to working memory capacity (Kane & Engle, 2002; Redick, 2014; Redick & Engle, 2011), but no association was observed with measures of neural variability.

In spite of our use of advanced acquisition (rapid TR) and analytic techniques, the current experiment was limited by several factors. First, the temporal nature of the HRF inherently eliminates more fine-grained analyses of neuronal spiking available with electroencephalography or magnetoencephalography, and potentially confounds increased activation (i.e., higher peak) with duration (i.e., increased PSC in late peak phase) due to the sluggish nature of the vasculature and hemodynamic response (Buxton, 2012). Thus, fMRI may be limited in the ability to truly assess sustained versus transient activity during proactive/reactive cognitive control (Braver et al., 2009; Irlbacher et al., 2014), even with the more rapid sampling scheme utilized in the current experiment.

Second, the inherent nature of the AX design (low probability B cue followed by low probability BX probe) ensures that the hemodynamic parameters associated with B probes are more challenging to reliably estimate relative to AX counterparts. However, (a) AY probes are also infrequent events and (b) increased variability for BX trials was also present in the behavioral data, suggesting that the source of neural variability for B probes is not purely statistical in nature. Finally, our a priori identification of the different HRF windows may not have been sensitive to individual differences in HRF shape and timing, or to the fact that previous studies have observed different temporal properties across brain regions (Handwerker, Ollinger, & D'Esposito, 2004). However, the current approach provides several advantages over the standard method of estimating a single beta coefficient corresponding to the amplitude of the hemodynamic response utilized in most fMRI studies.

In summary, current results highlight the flexible role of the aI/VLPFC in implementing both proactive and more reactive cognitive processes during the AX-CPT task. Increased activation of the right aI/VLPFC during the cue period was associated with reduced neural activity during the probe period, potentially suggesting individual differences in neural suppression. However, the instantiation of proactive cognitive control following B cues exhibited a high degree of individual variability, contrasted with relatively more consistent

cognitive strategies (i.e., lower behavioral and neural variability) following the presentation of A cues. Future studies are required to both replicate current findings and to better determine the individual differences that contribute to the variable pattern of neural responses observed during proactive cognitive control.

ACKNOWLEDGMENTS

ORCID

Andrew R. Mayer https://orcid.org/0000-0003-2396-5609

REFERENCES

Andersson, J. L., Skare, S., & Ashburner, J. (2003). How to correct susceptibility distortions in spin-echo echo-planar images: Application to diffusion tensor imaging. *NeuroImage*, *20*, 870–888.

Anticevic, A., Cole, M. W., Murray, J. D., Corlett, P. R., Wang, X. J., & Krystal, J. H. (2012). The role of default network deactivation in cognition and disease. *Trends in Cognitive Sciences*, *16*, 584–592.

Aron, A. R. (2011). From reactive to proactive and selective control: Developing a richer model for stopping inappropriate responses. *Biological Psychiatry*, *69*, e55–e68.

Aron, A. R., Behrens, T. E., Smith, S., Frank, M. J., & Poldrack, R. A. (2007). Triangulating a cognitive control network using diffusion-weighted magnetic resonance imaging (MRI) and functional MRI. *The Journal of Neuroscience*, *27*, 3743–3752.

Aron, A. R., Robbins, T. W., & Poldrack, R. A. (2014). Inhibition and the right inferior frontal cortex: One decade on. *Trends in Cognitive Sciences*, *18*, 177–185.

Barch, D. M., Carter, C. S., Braver, T. S., Sabb, F. W., Macdonald, A., III, Noll, D. C., & Cohen, J. D. (2001). Selective deficits in prefrontal cortex function in medication-naive patients with schizophrenia. *Archives of General Psychiatry*, *58*, 280–288.

Barch, D. M., Carter, C. S., MacDonald, A. W., III, Braver, T. S., & Cohen, J. D. (2003). Context-processing deficits in schizophrenia: Diagnostic specificity, 4-week course, and relationships to clinical symptoms. *Journal of Abnormal Psychology*, *112*, 132–143.

Barch, D. M., & Ceaser, A. (2012). Cognition in schizophrenia: Core psychological and neural mechanisms. *Trends in Cognitive Sciences*, *16*, 27–34.

Bartoli, E., Aron, A. R., & Tandon, N. (2018). Topography and timing of activity in right inferior frontal cortex and anterior insula for stopping movement. *Human Brain Mapping*, *39*, 189–203.

Beck, A. T., Steer, R. A., & Brown, G. K. (1996). *Manual for the Beck depression inventory-II*. San Antonio, TX: Psychological Corporation.

Blackman, R. K., Crowe, D. A., DeNicola, A. L., Sakellaridi, S., MacDonald, A. W., III, & Chafee, M. V. (2016). Monkey prefrontal neurons reflect logical operations for cognitive control in a variant of the AX continuous performance task (AX-CPT). *The Journal of Neuroscience*, *36*, 4067–4079.

Botvinick, M. M., Cohen, J. D., & Carter, C. S. (2004). Conflict monitoring and anterior cingulate cortex: An update. *Trends in Cognitive Sciences*, *8*, 539–546.

Brass, M., Derrfuss, J., Forstmann, B., & von Cramon, D. Y. (2005). The role of the inferior frontal junction area in cognitive control. *Trends in Cognitive Sciences*, *9*, 314–316.

Braver, T. S. (2012). The variable nature of cognitive control: A dual mechanisms framework. *Trends in Cognitive Sciences*, *16*, 106–113.

Braver, T. S., Paxton, J. L., Locke, H. S., & Barch, D. M. (2009). Flexible neural mechanisms of cognitive control within human prefrontal cortex.

Proceedings of the National Academy of Sciences of the United States of America, *106*, 7351–7356.

Buckner, R. L. (2013). The cerebellum and cognitive function: 25 years of insight from anatomy and neuroimaging. *Neuron*, *80*, 807–815.

Buckner, R. L., Andrews-Hanna, J., & Schacter, D. (2008). The brain's default network: Anatomy, function, and relevance to disease. *Annals of the New York Academy of Sciences*, *1124*, 1–38.

Buxton, R. B. (2012). Dynamic models of BOLD contrast. *NeuroImage*, *62*, 953–961.

Cai, W., Ryali, S., Chen, T., Li, C. S., & Menon, V. (2014). Dissociable roles of right inferior frontal cortex and anterior insula in inhibitory control: Evidence from intrinsic and task-related functional parcellation, connectivity, and response profile analyses across multiple datasets. *The Journal of Neuroscience*, *34*, 14652–14667.

Carter, C. S., & van Veen, V. (2007). Anterior cingulate cortex and conflict detection: An update of theory and data. *Cognitive, Affective, & Behavioral Neuroscience*, *7*, 367–379.

Chen, G., Saad, Z. S., Adleman, N. E., Leibenluft, E., & Cox, R. W. (2015). Detecting the subtle shape differences in hemodynamic responses at the group level. *Frontiers in Neuroscience*, *9*, 375.

Chikazoe, J., Jimura, K., Hirose, S., Yamashita, K., Miyashita, Y., & Konishi, S. (2009). Preparation to inhibit a response complements response inhibition during performance of a stop-signal task. *The Journal of Neuroscience*, *29*, 15870–15877.

Cieslik, E. C., Mueller, V. I., Eickhoff, C. R., Langner, R., & Eickhoff, S. B. (2015). Three key regions for supervisory attentional control: Evidence from neuroimaging meta-analyses. *Neuroscience and Biobehavioral Reviews*, *48*, 22–34.

Cohen, J. D., Barch, D. M., Carter, C., & Servan-Schreiber, D. (1999). Context-processing deficits in schizophrenia: Converging evidence from three theoretically motivated cognitive tasks. *Journal of Abnormal Psychology*, *108*, 120–133.

Cox, R. W. (1996). AFNI: Software for analysis and visualization of functional magnetic resonance neuroimages. *Computers and Biomedical Research*, *29*, 162–173.

Coxon, J. P., Stinear, C. M., & Byblow, W. D. (2006). Intracortical inhibition during volitional inhibition of prepared action. *Journal of Neurophysiology*, *95*, 3371–3383.

Derrfuss, J., Brass, M., Neumann, J., & von Cramon, D. Y. (2005). Involvement of the inferior frontal junction in cognitive control: Meta-analyses of switching and Stroop studies. *Human Brain Mapping*, *25*, 22–34.

D'Esposito, M., Postle, B. R., Jonides, J., & Smith, E. E. (1999). The neural substrate and temporal dynamics of interference effects in working memory as revealed by event-related functional MRI. *Proceedings of the National Academy of Sciences of the United States of America*, *96*, 7514–7519.

Dias, E. C., Bickel, S., Epstein, M. L., Sehatpour, P., & Javitt, D. C. (2013). Abnormal task modulation of oscillatory neural activity in schizophrenia. *Frontiers in Psychology*, *4*, 540.

Glover, G. H. (1999). Deconvolution of impulse response in event-related BOLD fMRI. *NeuroImage*, *9*, 416–429.

Gusnard, D. A., & Raichle, M. E. (2001). Searching for a baseline: Functional imaging and the resting human brain. *Nature Reviews. Neuroscience*, *2*, 685–694.

Handwerker, D. A., Ollinger, J. M., & D'Esposito, M. (2004). Variation of BOLD hemodynamic responses across subjects and brain regions and their effects on statistical analyses. *NeuroImage*, *21*, 1639–1651.

Ide, J. S., Shenoy, P., Yu, A. J., & Li, C. S. (2013). Bayesian prediction and evaluation in the anterior cingulate cortex. *The Journal of Neuroscience*, *33*, 2039–2047.

Irlbacher, K., Kraft, A., Kehrer, S., & Brandt, S. A. (2014). Mechanisms and neuronal networks involved in reactive and proactive cognitive control of interference in working memory. *Neuroscience and Biobehavioral Reviews*, *46*(Pt 1), 58–70.

Jahfari, S., Stinear, C. M., Claffey, M., Verbruggen, F., & Aron, A. R. (2010). Responding with restraint: What are the neurocognitive mechanisms? *Journal of Cognitive Neuroscience*, *22*, 1479–1492.

Kane, M. J., & Engle, R. W. (2002). The role of prefrontal cortex in working-memory capacity, executive attention, and general fluid intelligence: An individual-differences perspective. *Psychonomic Bulletin & Review*, *9*, 637–671.

Kern, R. S., Nuechterlein, K. H., Green, M. F., Baade, L. E., Fenton, W. S., Gold, J. M., ... Marder, S. R. (2008). The MATRICS consensus cognitive battery, part 2: Co-norming and standardization. *The American Journal of Psychiatry*, 165, 214–220.

Lesh, T. A., Westphal, A. J., Niendam, T. A., Yoon, J. H., Minzenberg, M. J., Ragland, J. D., ... Carter, C. S. (2013). Proactive and reactive cognitive control and dorsolateral prefrontal cortex dysfunction in first episode schizophrenia. *Neuroimage: Clinical*, 2, 590–599.

Leunissen, I., Coxon, J. P., & Swinnen, S. P. (2016). A proactive task set influences how response inhibition is implemented in the basal ganglia. *Human Brain Mapping*, 37, 4706–4717.

Lindquist, M. A., Meng, L. J., Atlas, L. Y., & Wager, T. D. (2009). Modeling the hemodynamic response function in fMRI: Efficiency, bias and mis-modeling. *NeuroImage*, 45, S187–S198.

Lopez-Garcia, P., Lesh, T. A., Salo, T., Barch, D. M., MacDonald, A. W., III, Gold, J. M., ... Carter, C. S. (2016). The neural circuitry supporting goal maintenance during cognitive control: A comparison of expectancy AX-CPT and dot probe expectancy paradigms. *Cognitive, Affective, & Behavioral Neuroscience*, 16, 164–175.

Mayer, A. R., Franco, A. R., Ling, J., & Canive, J. M. (2007). Assessment and quantification of head motion in neuropsychiatric functional imaging research as applied to schizophrenia. *Journal of the International Neuropsychological Society*, 13, 839–845.

Mayer, A. R., Teshiba, T. M., Franco, A. R., Ling, J., Shane, M. S., Stephen, J. M., & Jung, R. E. (2011). Modeling conflict and error in the medial frontal cortex. *Human Brain Mapping*, 33, 2843–2855.

Menon, V., & Uddin, L. Q. (2010). Saliency, switching, attention and control: A network model of insula function. *Brain Structure & Function*, 214, 655–667.

Miller, B. L., & Cummings, J. L. (2017). *The human frontal lobes: Functions and disorders*. New York, NY: Guilford Publications.

Morishima, Y., Okuda, J., & Sakai, K. (2010). Reactive mechanism of cognitive control system. *Cerebral Cortex*, 20, 2675–2683.

Niendam, T. A., Laird, A. R., Ray, K. L., Dean, Y. M., Glahn, D. C., & Carter, C. S. (2012). Meta-analytic evidence for a superordinate cognitive control network subserving diverse executive functions. *Cognitive, Affective, & Behavioral Neuroscience*, 12, 241–268.

Nuechterlein, K. H., Green, M. F., Kern, R. S., Baade, L. E., Barch, D. M., Cohen, J. D., ... Marder, S. R. (2008). The MATRICS consensus cognitive battery, part 1: Test selection, reliability, and validity. *American Journal of Psychiatry*, 165, 203–213.

Paxton, J. L., Barch, D. M., Racine, C. A., & Braver, T. S. (2008). Cognitive control, goal maintenance, and prefrontal function in healthy aging. *Cerebral Cortex*, 18, 1010–1028.

Paxton, J. L., Barch, D. M., Storandt, M., & Braver, T. S. (2006). Effects of environmental support and strategy training on older adults' use of context. *Psychology and Aging*, 21, 499–509.

Piepho, H. P. (1997). Tests for equality of dispersion in divariate samples-review and empirical comparison. *Journal of Statistical Computation and Simulation*, 56, 353–372.

Poppe, A. B., Barch, D. M., Carter, C. S., Gold, J. M., Ragland, J. D., Silverstein, S. M., & MacDonald, A. W., III. (2016). Reduced frontoparietal activity in schizophrenia is linked to a specific deficit in goal maintenance: A multisite functional imaging study. *Schizophrenia Bulletin*, 42, 1149–1157.

Rae, C. L., Hughes, L. E., Weaver, C., Anderson, M. C., & Rowe, J. B. (2014). Selection and stopping in voluntary action: A meta-analysis and combined fMRI study. *NeuroImage*, 86, 381–391.

Redick, T. S. (2014). Cognitive control in context: Working memory capacity and proactive control. *Acta Psychologica*, 145, 1–9.

Redick, T. S., & Engle, R. W. (2011). Integrating working memory capacity and context-processing views of cognitive control. *Quarterly Journal of Experimental Psychology*, 64, 1048–1055.

Richmond, L. L., Redick, T. S., & Braver, T. S. (2015). Remembering to prepare: The benefits (and costs) of high working memory capacity. *Journal of Experimental Psychology. Learning, Memory, and Cognition*, 41, 1764–1777.

Ridderinkhof, K. R., van den Wildenberg, W. P., Segalowitz, S. J., & Carter, C. S. (2004). Neurocognitive mechanisms of cognitive control: The role of prefrontal cortex in action selection, response inhibition, performance monitoring, and reward-based learning. *Brain and Cognition*, 56, 129–140.

Sebastian, A., Rossler, K., Wibral, M., Mobascher, A., Lieb, K., Jung, P., & Tuscher, O. (2017). Neural architecture of selective stopping strategies: Distinct brain activity patterns are associated with attentional capture but not with outright stopping. *The Journal of Neuroscience*, 37, 9785–9794.

Shenhav, A., Botvinick, M. M., & Cohen, J. D. (2013). The expected value of control: An integrative theory of anterior cingulate cortex function. *Neuron*, 79, 217–240.

Smith, S. M., Jenkinson, M., Woolrich, M. W., Beckmann, C. F., Behrens, T. E., Johansen-Berg, H., ... Matthews, P. M. (2004). Advances in functional and structural MR image analysis and implementation as FSL. *NeuroImage*, 23(Suppl 1), S208–S219.

Sridharan, D., Levitin, D. J., & Menon, V. (2008). A critical role for the right fronto-insular cortex in switching between central-executive and default-mode networks. *Proceedings of the National Academy of Sciences of the United States of America*, 105, 12569–12574.

Swann, N. C., Cai, W., Conner, C. R., Pieters, T. A., Claffey, M. P., George, J. S., ... Tandon, N. (2012). Roles for the pre-supplementary motor area and the right inferior frontal gyrus in stopping action: Electrophysiological responses and functional and structural connectivity. *NeuroImage*, 59, 2860–2870.

Swick, D., Ashley, V., & Turken, U. (2011). Are the neural correlates of stopping and not going identical? Quantitative meta-analysis of two response inhibition tasks. *NeuroImage*, 56, 1655–1665.

Talairach, J., & Tournoux, P. (1988). *Co-planar stereotaxic atlas of the human brain*. New York, NY: Thieme.

van den Wildenberg, W. P., Burle, B., Vidal, F., van der Molen, M. W., Ridderinkhof, K. R., & Hasbroucq, T. (2010). Mechanisms and dynamics of cortical motor inhibition in the stop-signal paradigm: A TMS study. *Journal of Cognitive Neuroscience*, 22, 225–239.

Wager, T. D., & Smith, E. E. (2003). Neuroimaging studies of working memory: A meta-analysis. *Cognitive, Affective, & Behavioral Neuroscience*, 3, 255–274.

Waskom, M. L., Kumaran, D., Gordon, A. M., Rissman, J., & Wagner, A. D. (2014). Frontoparietal representations of task context support the flexible control of goal-directed cognition. *The Journal of Neuroscience*, 34, 10743–10755.

Yang, Z., & Mayer, A. R. (2014). An event-related FMRI study of exogenous orienting across vision and audition. *Human Brain Mapping*, 35, 964–974.

Zandbelt, B. B., Bloemendaal, M., Hoogendam, J. M., Kahn, R. S., & Vink, M. (2013). Transcranial magnetic stimulation and functional MRI reveal cortical and subcortical interactions during stop-signal response inhibition. *Journal of Cognitive Neuroscience*, 25, 157–174.

Zandbelt, B. B., Bloemendaal, M., Neggers, S. F., Kahn, R. S., & Vink, M. (2013). Expectations and violations: Delineating the neural network of proactive inhibitory control. *Human Brain Mapping*, 34, 2015–2024.

Zandbelt, B. B., & Vink, M. (2010). On the role of the striatum in response inhibition. *PLoS One*, 5, e13848.

SUPPORTING INFORMATION

Additional supporting information may be found online in the Supporting Information section at the end of the article.